547905, 2022, 12, Downloaded from https://aiche.onlinelibtary.wiley.com/doi/10.1002/aic.17863, Wiley Online Library on [28/12/2022]. See the Terms and Conditions (https://onlinelibtary.wiley.com/terms-and-conditions) on Wiley Online Library for rules of use; OA articles are governed by the applicable Creative Commons License

DOI: 10.1002/aic.17863

RESEARCH ARTICLE

Reaction Engineering, Kinetics and Catalysis



Solvothermal liquefaction of waste polyurethane using supercritical toluene in presence of noble metal catalysts

Vahab Ghalandari Soudeh Banivaheb | Jessica Peterson Hunter Smith M. Toufig Reza

Department of Biomedical and Chemical Engineering and Sciences, Florida Institute of Technology, Melbourne, Florida, USA

Correspondence

M. Toufig Reza, Department of Biomedical and Chemical Engineering and Sciences, Florida Institute of Technology, 150 West University Boulevard, Melbourne, FL 32901, USA. Email: treza@fit.edu

Funding information

National Science Foundation, Grant/Award Number: 2123495

Abstract

Solvothermal liquefaction (STL) is a thermochemical conversion method that uses sub-or supercritical solvents to convert waste plastics like waste polyurethane (PU) into value-added chemicals. This study aimed to evaluate catalytic STL utilizing toluene as a solvent for depolymerization of waste PU into valuable products. The effect of catalyst type (Pt/C, Pd/C, and Ru/C), catalyst loading (0-10 wt%), STL reaction temperature (330°C, 350°C, and 370°C), STL residence time (1, 3, and 5 h), and hydrogen loading (25, 50, and 75 bar) on STL conversion were studied. Results showed that Ru/C outperformed Pt/C and Pd/C and the STL conversion reached to as high as 87.2%. The concentrations of nitrogen-containing components like aniline and p-aminotoluene were increased with the increase of Ru/C loading and STL reaction temperature.

KEYWORDS

depolymerization, noble metal catalysts, reaction mechanism, supercritical fluids, waste plastics

INTRODUCTION 1

Waste plastic has become a significant threat to the environment as more than 37 million tons of plastic wastes are produced annually in the United States. Polyurethane (PU, recycle class # 07) is one of the main contributors to these waste plastics along with polyethylene, polystyrene, polyamide, polyester, and others. Polyurethane, a thermoset, contains heteroatoms like nitrogen, and oxygen, and also contains aromatic rings, which result in a difficult and energy-intensive recycle of PU.² As a result, waste PU in the form of used mattresses, couches, car seats, and so on are destined to be landfilled. Depolymerization of waste PU can potentially redirect these wastes from landfills to manufacturing sectors.3

One of the rising thermochemical methods for combating the growing volume of plastic waste is hydrothermal liquefaction (HTL) that uses water as a solvent. Water is the most common green solvent in nature, and it has extremely distinct favorable characteristics in

sub- and supercritical conditions.⁴ During HTL, water acts as a reaction medium to help break down complex polymers into smaller molecules that repolymerize into biocrude that can be upgraded into liquid fuels.⁵ Temperature is a critical factor in the HTL process. While temperatures between 250°C and 400°C are regarded ideal for HTL, gas formation reactions are prominent at temperatures above 400°C, whereas carbonization reactions are dominating and solid product formation is strong at temperatures between 180°C and 250°C.^{6,7} While HTL has been predominantly performed for wet biowastes like sewage sludge, 8,9 animal manure, 10,11 and municipal solid waste, 12,13 it has also been reported for plastics. 14,15 In fact, the literature suggests that HTL could depolymerize PU and generate a liquid product rich in polyols and amines free from urethane bonds. ¹⁶ While HTL provides a more sustainable alternative for chemical production than other thermochemical processes like pyrolysis, the process still results in high heteroatom contents that prevent the direct use of the product. 17,18 HTL also introduces an expensive phase separation process, where nonpolar hydrocarbons are separated from the polar phase. Moreover, a significant portion of carbon from the feedstock is lost in the

Vahab Ghalandari and Soudeh Banivaheb contributed equally and share the first authorship.

GHALANDARI ET AL.

AICHE 2 of 11

aqueous phase, which results in lowering the carbon recovery. Additionally, water has a relatively higher critical temperature and higher critical pressure than many other polar and nonpolar solvents like ethanol, methanol, toluene, hexane, and so on.

On the other hand, solvothermal liquefaction (STL) offers higher quality products with less likelihood of heteroatom contents. STL has a similar working principle as HTL, except the solvent used for STL is not water. STL uses lower reaction temperatures than HTL that may lower the operating costs. It also does not lose carbon in the aqueous phase. Thus far, different solvents have been used in the STL process including toluene, propanol, acetone, ethanol, and methanol to generate fuels from wastes. 19 While recent studies have illustrated that the oxygenated solvents may be inappropriate for a broad range of fuel-based utilization, 20-22 our group has recently revealed that toluene, a nonoxygenated solvent, is an appropriate STL solvent to produce liquid fuels from waste plastics.²³ Toluene is a hydrogen donor solvent with lower critical temperature and lower critical pressure compared with water.²⁴ Using a hydrogen-donor solvent can help to stabilize the free radicals produced, and reduce the repolymerization reaction significantly.²⁵ Tetralin, for example, is another example of hydrogen donor solvent, and one fuel study showed that hydrogen transferred from tetralin has a considerable impact on oil vield.²⁶ Moreover, supercritical toluene turns out to be effective in depolymerizing waste plastics.²⁴ However, the STL conversion was relatively lower as many of the chemical bonds in plastics are strong enough to withstand the supercritical toluene atmosphere. Noble metal catalysts, such as platinum, palladium, and ruthenium could enhance depolymerization in the form of hydrodeoxygenation and ringopening mechanisms.^{27,28} These noble metal catalysts have previously been used with chemical plastic recycling, such as using ruthenium in the STL process for polyethylene.²⁹ Ruthenium in carbon (Ru/C) in presence of hydrogen has been shown to break hydrocarbons into shorter chains and cleave the C-C bond to create high-value chemicals. 30,31 Hydrogen is often employed with noble metal catalyst to enhance the depolymerization of plastics, as it could promote deoxygenation reaction.³² Moreover, the production of saturated C-C bonds from the interaction of oxygen and hydrogen boosts the liquid product stability and decreases its acidity level, and viscosity.33

The main goal of this study was to evaluate the STL of waste PU using supercritical toluene in presence of various noble metal catalysts. STL experiments were performed to determine the effect of catalyst type, catalyst loading, reaction temperature, residence time, and hydrogen loading on depolymerization of waste PU. STL products were characterized to determine the chemical changes during STL reactions, and valuable chemicals were shortlisted from the depolymerization of waste PU. Finally, a reaction mechanism was proposed for catalytic STL of waste PU.

2 | MATERIALS AND METHODS

2.1 | Materials

A commercial mattress was used as the source of waste PU. Reagent grade toluene was purchased from Fisher Scientific (Waltham,

Massachusetts). Two of the catalysts, type 490 palladium 5 wt% on carbon powder (Pd/C) and platinum 5 wt% on carbon (Pt/C) were purchased from Alfa Aesar (Ward Hill, Massachusetts). The third catalyst, ruthenium 5 wt% on activated carbon powder (Ru/C) was purchased from Fisher Scientific (Waltham, Massachusetts). Finally, nitrogen and hydrogen gases were purchased from NexAir (Melbourne, Florida).

2.2 | Solvothermal liquefaction

A 25 ml stainless steel (SS-316) Parr batch reactor (Moline, Illinois) was used to perform the catalytic STL experiments. The experiments were performed with varying catalyst types, catalyst loading, STL temperature, residence time, and hydrogen loading. In a typical STL experiment, waste PU, catalyst, and toluene were fed into the reactor to maintain a ratio of 1:10 (solid weight:toluene weight).²³ The reactor was purged with nitrogen gas for three times to remove air from the reactor headspace. Hydrogen was then loaded into the reactor after purging the reactor with hydrogen three times. The sealed reactor was heated using a preheated Techne SBL 1 sand bath (Long Branch, New Jersey) at the set STL temperature. As soon as the residence time was finished, the reactor was taken out from the sand bath and cooled by natural convection. Once cooled, the gaseous products were vented in a fume hood. Afterwards, the contents of the reactor were filtered through a 1 µm glass fiber syringe filter purchased from Tisch Scientific (North Bend, Ohio). After filtration, the syringe filter was first dried at the fume hood and then in an oven at approximately 105°C overnight to determine the STL conversion.

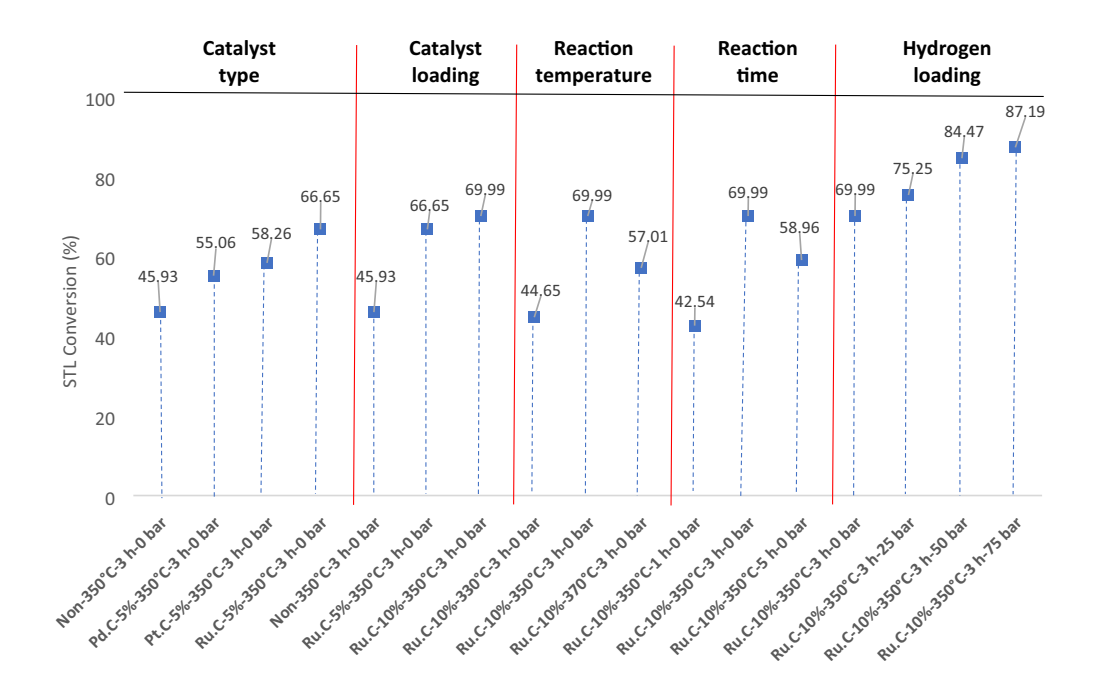
$$STL \, conversion = \left(1 - \frac{\text{weight of dried solid after STL}}{\text{weight of waste PU}}\right) \times 100\% \quad (1)$$

2.3 | Characterization of STL liquid products

The Flash 1112 Organic Elemental Analyzer from Thermo Scientific (Waltham, Massachusetts) was utilized to complete the ultimate analysis in triplicate. Because the STL products were dissolved in toluene, toluene was first removed from a portion of the mixture (about 20 μ l) using natural convection on an aluminum sample pan, and then the leftover was prepared with other standards. 2,5-Bis(5-tert-butyl-benzoxazol-2-yl) thiophene (BBOT) was utilized as a calibration standard, and vanadium oxide (V2O5) was utilized as a conditioner for the samples. The samples were oxidized at 950°C in ultra-high purity oxygen with a helium carrier gas and passed over copper oxide pellets and then electrolytic copper. The gases were then tested using a thermal conductivity detector (TCD), and the detection peak regions for CHNS were compared with BBOT parameters. The oxygen content was determined by calculating the difference.

FTIR analysis was carried out in a Nicolet iS5 Thermo Scientific FTIR (Madison, Wisconsin) to identify functional groups in the STL products. Because the product was dissolved in toluene, one droplet of the mixture was poured on an IR card and waited until the toluene

FIGURE 1 The effect of catalyst type, catalyst loading, reaction temperature, reaction time, and hydrogen loading on the STL conversion.



was evaporated naturally. The operating conditions were set as follows: data accumulation: 64, resolution (4), and wavenumber range $(500-4000 \text{ cm}^{-1})$.

Gas chromatography–mass spectrometry (GCMS) was used to chromatograph the STL products using an Agilent 7890 GC combined with a 5975 Mass Spectrometer. A Supelco Equity 1701 column (60 m \times 0.25 mm \times 0.25 m) was used for GCMS. The column was first held at 250°C with a split ratio of 1:1 and inert helium flow of 5 ml/min. The oven was preheated to 45°C for 4 min, then increased to 280°C at a rate of 3°C/min for 20 min. All samples were doped (0.1 wt%) with an internal standard (n-decane, 99% MilliporeSigma) with no overlapping chromatogram peaks before injection.

3 | RESULTS AND DISCUSSION

3.1 | STL conversion of waste polyurethane

Initial catalyst screening was performed by conducting STL experiments using Pd/C, Pt/C, and Ru/C catalysts at 3 h residence time at 350°C and a loading catalyst percentage of 5 wt%. The initial operation temperature and residence time were considered based on our recent study.²³ This method enabled the selection of catalyst for further STL reactions. The results are presented in Figure 1. It can be seen that the inclusion of all three catalysts promotes STL conversion in an inert environment. Similar findings were reported in the literature,³⁴ but with water as the solvent. In this STL study with toluene, a 5 wt% Ru/C produces the highest STL conversion (66.65%), which is 8.39% higher than 5 wt% Pt/C and 11.59% higher than 5 wt% Pd/C. Changing Ru/C catalyst loading from 0 to 10 wt% has also shown an increasing STL conversion of waste PU.

To evaluate the effect of STL reaction temperature on STL conversion of waste PU, STL reaction temperature was varied from 330° C to

370°C with 10% Ru/C loading. The results shown in Figure 1 indicate that STL reaction at 350°C had the highest conversion (70.0%) compared with the STL at 330°C (44.6%) and 370°C (57.0%). This is most likely due to the 330°C being too close to the toluene's supercritical temperature to effectively break the polyurethane into smaller polymer chains and having slower reaction kinetics, while 370°C could be too high and either result in a reversible exothermic reaction or repolymerize the large number of reaction intermediates into a solid.³⁵ In fact, Jia et al.,²⁹ observed a similar trend for high-density polyethylene (HDPE) in an STL process, which used n-hexane as solvent. They found no depolymerization at 150°C. The maximum depolymerization was carried out at 200°C, and after this temperature, the yield of depolymerization significantly decreased due to a possible repolymerization. A similar trend on STL conversion was observed in this study at various STL reaction times at constant STL temperatures of 350°C and 10% Ru/C loading, where the highest STL conversion was observed for 3 h compared with that of 1 and 5 h of STL residence time when the other STL reaction parameters remained the same. This could be due to 1 h residence time not being long enough to fully depolymerize the waste PU, and that the 5 h residence time provides enough time for the liquid phase to repolymerize the depolymerized chains into the solid phase.²⁹ Literature also reported a similar observation where HDPE was rapidly degraded to liquid hydrocarbons in hexane in only 0.5 h at 220°C.²⁹ The maximum yield in the literature was achieved in 1 h, and almost no high-molecular-weight products were observed after 1 h.

The effect of hydrogen loading was then investigated by performing a set of STL experiments at 350°C, 3 h, and in presence of 10 wt% Ru/C catalysts with an initial hydrogen loading of 25, 50, and 75 bar. Figure 1 illustrates that adding high-pressure hydrogen to the reactor increases the STL conversion significantly. The STL conversion is found to be as high as 87.2% when 75 bar of hydrogen was added. The hydrogen most likely assists in the deoxygenation, which could break the molecules down and depolymerizes the PU.³⁶ A similar

TABLE 1 Ultimate analysis of STL products prepared at various STL conditions

Catalyst	Catalyst loading (%)	Temperature (°C)	Time (h)	Hydrogen loading (bar) ^a	Carbon (%)	Hydrogen (%)	Nitrogen (%)	Oxygen (%)
None (Control)	0	350	3	0	52.21 ± 0.18	7.25 ± 0.00	5.95 ± 0.05	34.59 ± 0.22
Pd/C	5	350	3	0	56.92 ± 0.00	8.23 ± 0.00	2.92 ± 0.00	31.93 ± 0.00
Pt/C	5	350	3	0	56.76 ± 1.26	8.03 ± 0.19	2.99 ± 0.11	32.22 ± 1.55
Ru/C	5	350	3	0	55.44 ± 0.35	7.63 ± 0.05	3.75 ± 0.03	33.19 ± 0.43
Ru/C	10	350	3	0	65.41 ± 0.95	9.64 ± 0.17	2.29 ± 0.03	22.66 ± 0.75
Ru/C	10	330	3	0	50.27 ± 0.13	11.33 ± 0.03	1.22 ± 0.03	37.18 ± 0.19
Ru/C	10	370	3	0	54.14 ± 0.85	10.68 ± 0.13	2.61 ± 0.06	32.56 ± 1.04
Ru/C	10	350	1	0	51.18 ± 0.66	11.09 ± 0.21	1.52 ± 0.01	36.21 ± 0.87
Ru/C	10	350	5	0	67.21 ± 0.64	5.82 ± 0.15	5.99 ± 0.1	21.01 ± 0.87
Ru/C	10	350	3	25	50.85 ± 0.91	10.32 ± 0.18	2.50 ± 0.17	36.33 ± 0.92
Ru/C	10	350	3	50	51.55 ± 0.13	10.83 ± 0.02	1.99 ± 0.07	35.63 ± 0.22
Ru/C	10	350	3	75	53.77 ± 1.02	11.09 ± 0.33	2.22 ± 0.30	32.92 ± 1.04

^a0 bar means only no hydrogen.

effect was observed in the literature, where hydrogen loading had a significant effect on the HDPE depolymerization in presence of Ru/C.²⁹

Elemental compositional analysis of STL liquid products

Ultimate analysis was performed to determine elemental carbon, hydrogen, nitrogen, sulfur, and oxygen in the STL liquid products, and the results are presented in Table 1. Regardless of catalyst type, catalytic STL showed to have a higher carbon content than the control STL (by at least 3% higher). However, the increase in STL temperature (from 350°C to 370°C) reveals a significant decrease in carbon content (11.3%) and increase in oxygen content (9.9%). The decrease in STL temperature (from 350°C to 330°C) shows a significant decrease in carbon content (15.1%) and increase in oxygen content (14.5%). Hydrogen content was also decreased, and nitrogen content was increased significantly with the addition of catalysts. A similar trend was reported in a catalytic HTL study when Ru/C and Pt/C were used.³⁷ Possible reasons for this observation could be the reaction kinetics are slower at 330°C, and it seems that a reversible exothermic reaction or reaction intermediates repolymerizing into a solid phase occurs for the 370°C.38 Moreover, 1 h STL reaction time yields a lower STL conversion than the 3 and 5 h reaction time, as well as 14.2% and 15.1% decrease in carbon, and 13.5% and 14.2% increase in oxygen content than the 3 and 5 h, respectively, which could possibly indicate that 1 h STL at 350°C is inadequate to complete the reaction.³⁹ Also, by increasing the reaction time, the nitrogen content increases, and hydrogen content decreases significantly.

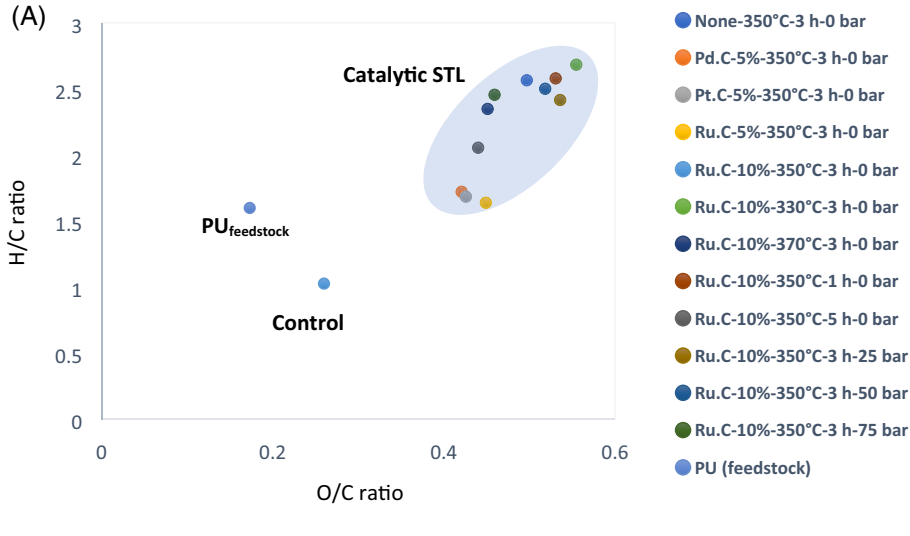
The carbon content was also decreased by an average of 13% when hydrogen loading was increased. Not surprisingly, the hydrogen percentage was also increased from 5.6% (control) to 11.1% for 75 bar of hydrogen loading. Furthermore, the oxygen content was increased and nitrogen content was decreased with the increase of hydrogen loading prior to STL. A set of Van Krevelen diagram⁴⁰ was drawn for STL liquid products and shown in Figure 2. It illustrates how the atomic O/C and atomic H/C or N/C ratios of the STL liquid product samples change with reaction conditions and how they vary from waste PU. STL of waste PU produced a liquid product that has a higher O/C ratio than the waste PU because of the amount of oxygen and carbon in the liquid product samples are increased and decreased, respectively. Figure 2A shows that the H/C ratio increases in STL liguid products since their hydrogen amount increases with STL. In addition to reaction conditions, previous research proved that H/C and O/C ratios changing are strongly related to the type of plastics. For instance. Seshasavee and Savage³⁵ found HTL of polypropylene produces a liquid product that has the higher O/C and lower H/C than the feedstock while HTL of polyethylene terephthalate produces a liguid product that has lower O/C and higher H/C than the feedstock. The N/C ratio decreases in STL liquid products in compared with the raw PU. Liu et al.⁴¹ found the similar trend where they used STL method to depolymerize polyethylene. It can be seen on Figure 2B that the catalysts have a significant effect to decrease the nitrogen through STL. Bai et al.⁴² reported that Pt/C, Pd/C, and Ru/C are able to reduce the N/C ratio considerably through HTL process.

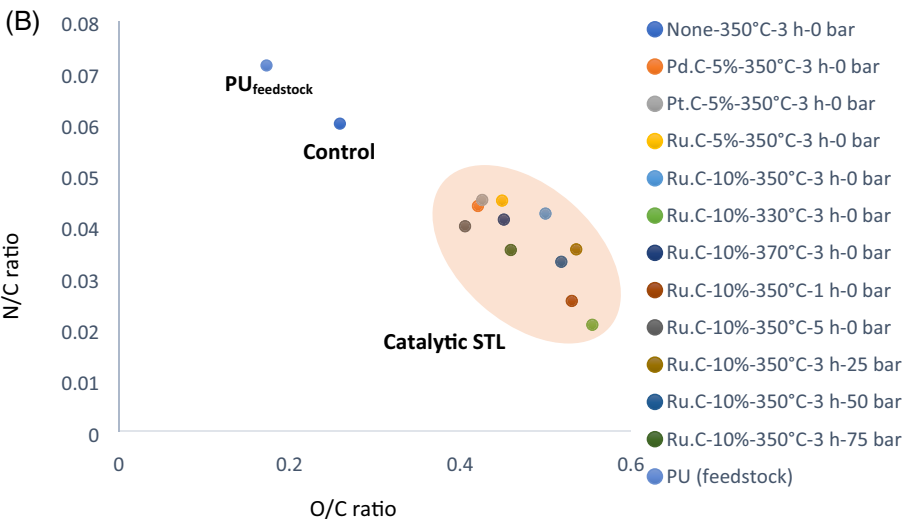
FTIR analysis of STL liquid products 3.3

The FTIR spectra of STL liquid products enable molecular structure and predominant bonds.⁴³ Therefore, the FTIR analysis of all STL liquid samples were performed at wavenumbers of 400-4000 cm⁻¹. As shown in Figure 3, all STL liquid samples have identical peaks apart from a few minor changes in peaks. The peaks in the range of 640-700 cm⁻¹ demonstrate the existence of C=C bending, and the peaks in the range of 795-1170 cm⁻¹ demonstrate stretching of C-O (aliphatic ether), and -OHC groups in the STL liquids. 44 The sharp peak at \sim 710 cm⁻¹ demonstrates the existence of benzene derivatives in liquid samples that is in line with GC-MS results (discussed

5475905, 2022, 12, Downloaded from https://aiche.onlinelibrary.wiley.com/doi/10.1002/aic.17863, Wiley Online Library on [28/12/2022]. See the Terms and Conditions (https://onlinelibrary.wiley.com/terms-and-conditions) on Wiley Online Library for rules of use; OA articles are governed by the applicable Creative Commons. Licenses

FIGURE 2 Van Krevelen diagram of catalytic STL products and raw PU feedstock.





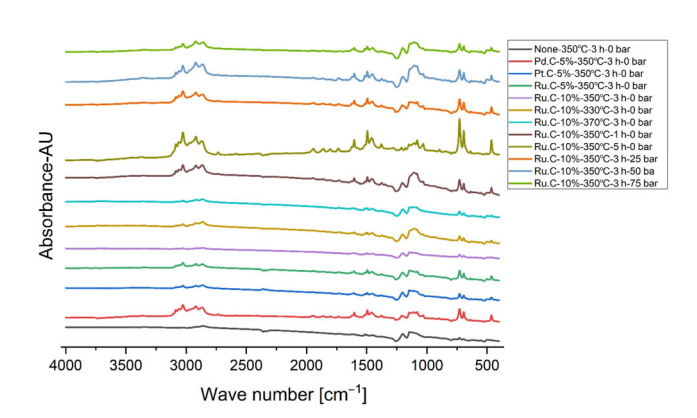


FIGURE 3 FTIR analysis of STL products produced at various STL reaction conditions.

later). The strong peak at \sim 1250 cm⁻¹ represents that a C-O stretching (aromatic ester) is existing in STL liquids. There are some peaks in the range of 1380–1470 cm⁻¹ and 1750–1850 cm⁻¹ that are related to the existence of alkane and aromatic components (C-H bending) in the STL liquids. The existence of a peak at 1540 cm⁻¹, and some peaks in the range of 1650–1700 cm⁻¹ can be related to N-O stretching, and C=C bonding, respectively. Some peaks can be

observed in the range of $1700-1710~\text{cm}^{-1}$ which can be related to the presence of aliphatic ketone. The presence of aliphatic hydrocarbons in the long chain is indicated by the C-H stretching peak within the $2800-3000~\text{cm}^{-1}$ region. Finally, for all liquid samples, a minor peak indicating alkanes were present at roughly $3000~\text{cm}^{-1}$ (due to C-H stretching of $-\text{CH}_3$, $-\text{CH}_2$, and -CH).

3.4 | Chemical composition of catalytic STL liquid products

GCMS was used to identify molecular components in STL liquid products from catalytic STL in a hydrogen atmosphere. Figure 4 compares the effect of different catalysts on the total area percentage of the different compound with catalyst type. The detailed results of GCMS analysis are presented in Appendix S1. All of the catalysts have a positive effect on decreasing the oxygen content that has been supported by previous studies. ^{47–49} In a comparison of various catalyst types, it can be found that Pd/C, Ru/C, and Pt/C catalysts produce aliphatic and aromatic compounds of about 71%, 67%, and 59%, respectively. However, when compared among the catalysts used in this study, the

GHALANDARI ET AL.

AICHE 6 of 11
JOURNAL

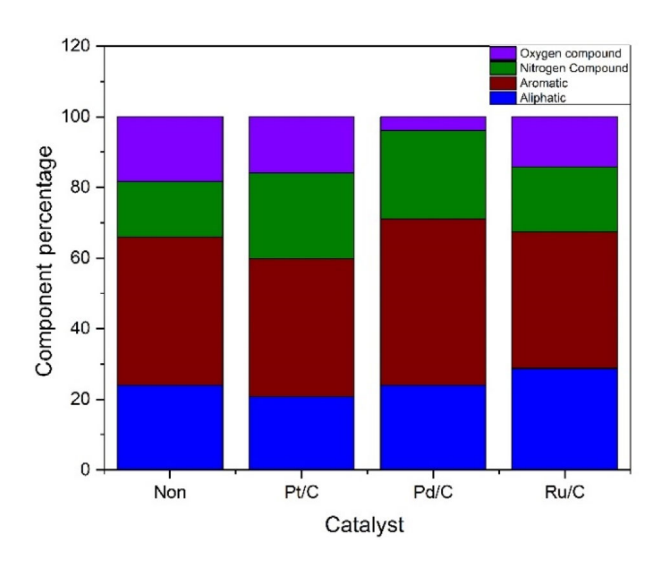


FIGURE 4 Effect of different catalysts on total identified area of different chemical compounds present in the STL liquid products (STL performed at 350°C for 3 h with 5% catalyst loading and no hydrogen loading).

Pd/C catalyst produced a lesser percentage of oxygen-containing compounds (only around 3%). As a result, it may be stated that the Pd/C catalyst is more effective for reducing oxygen compounds. Tridecane was the only aliphatic compound in all catalyzed samples, and it was higher than the others with the Ru/C catalyst which is about 28%. The major aromatic compounds in these trials were ethylbenzene, xylene, and 1,3-dimethyl-benzene.

Figure 5 depicts the influence of STL temperature on various compounds. Higher STL temperature causes to decrease in the aromatic and aliphatic compounds, which includes 60% of the products STL performed at 330°C. However, more nitrogen- and oxygencontaining compounds were produced with the increase of STL temperature. This could be due to a higher percentage of depolymerization, breaking down compounds into their aromatic components and breaking down aliphatic compounds. The generation of lighter oxygen compounds like cyclopentanone, 2-ethyl-and 2-methyl cyclopentanone, and valuable nitrogen compounds like aniline and p-aminotoluene could also be a cause. However, a higher temperature (e.g., 370°C) also breaks down the generated molecules at lower STL temperatures, and hydrocarbons are increased again. This positive effect of STL temperature has also been observed in the literature. 50,51 It indicates that a higher STL temperature might be favorable for hydrocarbon formation.

The impact of hydrogen loading on various compounds is depicted in Figure 6. It is prominent that with the addition of hydrogen (only 25 bar), the percentage of nitrogen compound is increased as the aniline and *p*-aminotoluene are increased roughly about 27% and 43% as well as production of new compounds like *n*-ethyl-benzeneamine, 3,4-dimethyl-benzeneamine, and *n*-ethyl-*p*-toluidine. However, higher hydrogen loading (e.g., 75 bar) yields a higher percentage of hydrocarbons than that of 25 and 50 bar of hydrogen loading. At 50 bar of hydrogen loading, the percentage of aniline decreased from

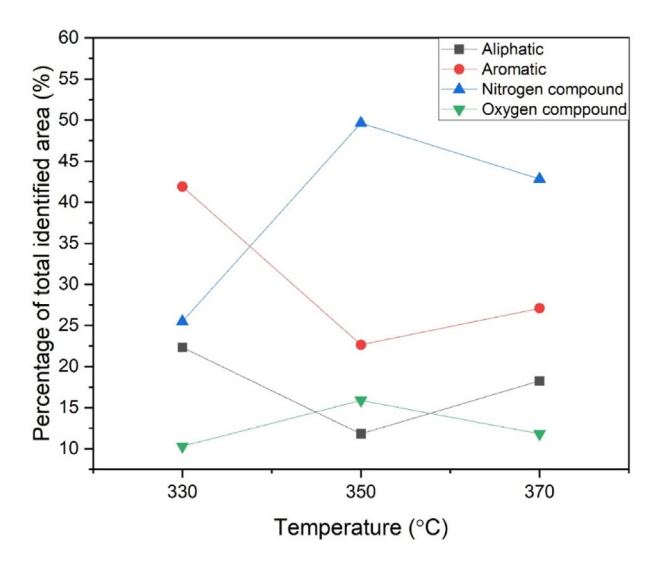


FIGURE 5 Effect of STL temperature on total identified area of different chemical compounds present in the STL liquid products (STL reaction condition: varied STL reaction temperature, 3 h reaction time, 10 wt% Ru/C, and no hydrogen loading).

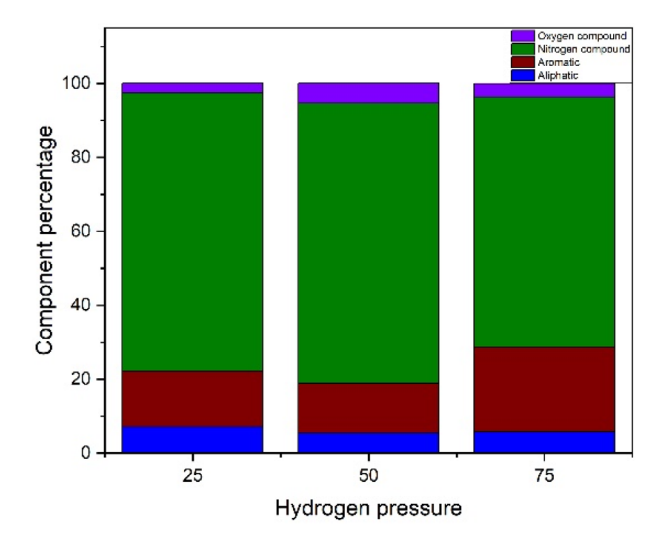


FIGURE 6 Effect of hydrogen loading on total identified area of different chemical compounds present in the STL liquid products (STL reaction condition: STL reaction temperature of 350°C, reaction time of 3 h, 10 wt% Ru/C, and varied hydrogen loading).

25 bar of hydrogen loading, however, the percentage of other components like *n*-ethyl-*p*-toluidine increased by about 56%. In addition, introducing hydrogen reduced the number of aliphatic molecules like tridecane. It is also worth noting that the percentage of *p*-xylene is nearly eliminated at 75 bar of hydrogen loading, whereas 1,3-dimethyl-benzene is not identified at 25 and 50 bar of hydrogen loading.

From the GCMS results, it can be noticed that several valuable nitrogen compounds are formed during catalytic STL with hydrogen loading. In Table 2, selective valuable nitrogen-containing, and aromatic compounds are listed which are produced during different

	Area percen	tage (%)			
Component	H ₂ (25 bar)	H ₂ (50 bar)	H ₂ (75 bar)	Applications	References
Aniline	29.48	22.12	17.23	Rubbers, pesticides, and dyes	[53]
p-Aminotoluene	33.76	33.73	30.56	Production of dyes and accelerators for cyanoacrylate glues	[54]
3,4-Dimethyl-benzenamine	4.07	5.24	6.17	Production of vitamin B2, dyes, pesticides	[55]
N-ethyl-p-toluidine	1.82	4.15	2.19	Chemical reagent	[56]
Ethylbenzene	6.23	4.46	4.33	Production of styrene	[57]
o-Xylene	6.75	_	-	To produce phthalic anhydride	[58]
p-Xylene	_	4.95	0.43	Circuit boards, sensors, LEDs	[59,60]
Diphenylmethane	0.34	0.94	5.57	The synthesis of luminogens for aggregation-induced emission (AIE) and used in the preparation of a polymerization initiator, diphenylmethyl potassium (DPMK)	[61]
Fluorene	1.33	3.47	4.34	To make dyes, plastics, and LED	[62-64]

hydrogen loading at STL. Aniline and p-aminotoluene are the main components in the STL liquid products. Aniline is a commercial chemical of industrial significance and a platform chemical for precision chemical synthesis. 52 Its primary application is in the production of precursors of polyurethane, dves, and other industrial chemicals. 53 The p-toluidine is a chemical intermediate used in the synthesis of dyes, organic molecules, and aromatic azo compounds.⁵⁴ It is a component of cyanoacrylate glue accelerators. It interacts with catecholamine to generate a dye that may be used to determine catecholamine medications.⁵⁴ The applications of other components are presented in Table 2. As discussed, by changing the STL operation conditions, the amount of each component could be changed. For example, when the hydrogen loading increases, the amount of diphenylmethane, fluorene, and 3,4-dimethyl-benzenamine increases, but the amount of aniline, p-aminotoluene, and ethylbenzene decrease. Toluene is suspected to be the major reactant that forms ethylbenzene, p-xylene, o-xylene, and 1,3-dimethyl benzene through radical aromatic substitution of methyl groups. The large amount of methyl radicals formed from thermolysis can react with the toluene radicals in the system to form the four major aromatic products of the reaction. The radical toluene can also form p-toluidine and o-toluidine by radical aromatic substitution of ammonia through a similar process.

3.5 | Proposed STL reaction mechanism

To understand the STL reaction mechanism of waste PU, the GCMS results were studied, and a possible reaction mechanism is proposed in Figure 7. The first stage of the STL is suspected to be caused by thermolysis of urethane linkages followed by decarboxylation of the carboxylic acid functional group to form CO₂. ⁶⁵ The use of toluene as a solvent in this reaction serves as a hydrogen donor to the free radicals formed due to homolysis. ⁶⁶ This splits the polymer into two major sections, the aromatic section, and the aliphatic section. The aliphatic group is suspected to form an alkene due to homolysis occurring at

both ends and a lack of hydrogen to saturate the hydrocarbon. The aromatic group undergoes further thermolysis into a base product of aniline and *p*-aminotoluene. The major aromatic products are formed via aromatic substation of aniline, followed by the removal of the amine group via homolysis.

The addition of Ru/C catalyst to STL did not result in a significant differentiation between products compared with the control run based on the GCMS data. However, Ru/C is suspected to increase the rate of decomposition for polyurethane based on the IR spectroscopy of the solid char Figure S7. With no catalyst, there is a clear IR peak at 3300 cm⁻¹ indicative of a secondary amine and another IR peak at 1740 cm⁻¹ indicative of an ester bond. These peaks are indicators of a urethane linkage in the solid char, which would imply that the polyurethane was not fully decomposed. The peaks of the IR in the control run are similar to that of other polyurethane IR graphs.⁶⁷ The secondary amine peak disappears with the addition of a catalyst, which is indicative of complete decomposition of polyurethane. The Ru/C catalyst serves primarily as a hydrogenation catalyst, which can quickly quench free radicals with hydrogen to prevent radical recombination during the reaction. Ru/C is most effective with hydrogen loading because the hydrogen gas can be used as a reactant during a metathesis reaction to saturate a double bond with hydrogenation.⁶⁸ In presence of Ru/C, dehydration of ethanol into ethene can occur, from which radical polymerization can occur resulting in higher amounts of aliphatic chain.69

Due to ethanol not being a substantial product in any of the liquid products, it is proposed that the ethanol products react extremely quickly when produced. The solid char mechanism implies that the majority of the solid product are aliphatic compounds due to the clear peak at 2900 cm⁻¹, typically associated with C-H stretch bonds in alkyl compounds. The amount of C=C bonds decreases significantly with the addition of a catalyst, and the percentage of C-O decreases, although the peak still remains in the spectrum. Because the secondary amine functional group disappears while the ester peaks remain, it can be assumed that after the urea bond breaks, the carboxyl group can react with aliphatic groups in order to become a component in

[5475905, 2022, 12, Downloaded from https://aiche.onlinelibrary.wiley.com/doi/10.1002/aic.17863, Wiley Online Library on [28/12/2022]. See the Terms

and-conditions) on Wiley Online Library for rules of use; OA articles are governed by the applicable Creative Commons License

Proposed STL reaction mechanism of waste PU under supercritical toluene (A: with no catalyst/hydrogen loading, B: with Ru/C catalyst, and C: with Ru/C catalyst and hydrogen loading).

the solid char. The suspected reaction that could occur is either termination or initiation of radical polymerization that occurs after thermolysis while the carboxyl group is still a free radical. Other components in the solid char include aliphatic chains produced from polymerization and undegraded polyurethane in the control group.

Hydrogen loading could help limit the number of aromatic compounds being formed in the products by saturating the aromatic rings. Based on the GCMS results, the aromatic products increase significantly, meaning that it is unlikely that the aromatic rings are saturated with carbon during the reaction. An increase in aromatization under Ru/C is unlikely due to Ru/C serving as a reduction catalyst, while aromatization would require an oxidative catalyst. 70 The proposed purpose of the hydrogen is therefore to limit the reaction rate of certain decomposition methods by saturating homolyzed bonds quickly after homolysis. This lowers the amount of potential radical initiators

for polymerization to higher alkanes. The presence of hydrogen also slowed down the production of ammonia in the system by making the gas production less thermodynamically favorable. The significant decrease in alkanes in the liquid component can be explained by the hydrogen quickly saturating the alkanes to prevent large chain polymerization from occurring through radicalization. The slowing down of the reaction allows for the formation of higher carbon aromatics such as fluorene and diphenylmethane. According to the GCMS data, the majority of products in presence of hydrogen contain nitrogen. The suspected reason for this is that at higher pressure, the formation of ammonia gas is less favorable than under the previous reaction conditions. The addition of hydrogen in the reactor resulted in an increase in the amount of n-alkylation. Ru/C has been shown to effectively perform n-alkylation in the presence of alcohol through the "hydrogen borrowing method." A possible explanation is that

ethanol is unlikely to remain formed for very long periods without the use of hydrogen to quickly saturate the oxygen radical product.

CONCLUSIONS

In this work, the impact of catalyst type, catalyst loading, reaction temperature, residence time, and hydrogen loading on the STL of waste polyurethane in the presence of supercritical toluene were observed. Pd/C, Pt/C, and Ru/C catalysts increase the STL conversion significantly, and the Ru/C has shown the highest STL conversion. In addition, increasing the catalyst loading (Ru/C) led to higher STL conversion and less oxygen content in the STL liquid product. The hydrogen loading improves the STL conversion sharply because it most likely assists in the deoxygenation, which broke the molecules down and depolymerized the polyurethane, and provides a more powerful environment that depolymerized the polyurethane. Hydrogen loading assisted the number of aromatic compounds being formed in the products by saturating the aromatic rings. Toluene was a hydrogen donor in this process, which split the polymer into aromatic and aliphatic sections. The amount of aromatic and nitrogen-containing components is the highest with 5 wt% Pd/C and the lowest with 5 wt% Ru/C. The STL conversion and number of nitrogen-containing components, especially aniline, are increased with increasing Ru/C loading.

AUTHOR CONTRIBUTIONS

Vahab Ghalandari: Conceptualization (equal); data curation (equal); formal analysis (equal); writing - original draft (equal); writing - review and editing (equal). Soudeh Banivaheb: Data curation (equal); formal analysis (equal): writing - original draft (equal), Jessica Peterson: Conceptualization (equal); formal analysis (equal); writing - original draft (equal). Hunter Smith: Formal analysis (equal); writing - original draft (equal). M. Toufiq Reza: Conceptualization (equal); funding acquisition (equal); project administration (equal); writing - review and editing (equal).

ACKNOWLEDGMENTS

This invited contribution is part of the 2022 Future Issue of AIChE Journal. The material is based upon work partially supported by National Science Foundation under Grant No. 2123495. The authors also acknowledge Andrew Wagner from Mainstream Engineering Corporation for assisting with GCMS.

DATA AVAILABILITY STATEMENT

The data that support the findings of this study are available from the corresponding author upon reasonable request.

ORCID

M. Toufiq Reza https://orcid.org/0000-0001-9856-5947

REFERENCES

1. Statista. Plastic Waste Generation Worldwide by Country. Accessed April 26, 2022. https://www.statista.com/statistics/1166177/plasticwaste-generation-of-select-countries/

- 2. Advanced Science News. A New Method to Chemically Recycle Polyurethane Waste. Accessed April 26, 2022. https://www. advancedsciencenews.com/solution-for-polyurethane-waste
- 3. Jiang J, Shi K, Zhang X, et al. From plastic waste to wealth using chemical recycling: A review. J Environ Chem Eng. 2022;10(1):106867. doi:10.1016/j.jece.2021.106867
- 4. Durak H. Hydrothermal liquefaction of Glycyrrhiza glabra L. (Liquorice): effects of catalyst on variety compounds and chromatographic characterization. Energy Sources Part A. 2020;42(20):2471-2484. doi:10.1080/15567036.2019.1607947
- 5. Peterson A, Vogel F, Lachance R P, et al. Thermochemical biofuel production in hydrothermal media: A review of sub- and supercritical water technologies. Energy Environ Sci. 2008;1(1):32-65. doi:10.1039/B810100K
- 6. Durak H, Genel S. Characterization of bio-oil and bio-char obtained from black cumin seed by hydrothermal liquefaction: investigation of potential as an energy source. Energy Sources Part A. 2020;1-11. doi: 10.1080/15567036.2020.1714821
- 7. Durak H. Characterization of products obtained from hydrothermal liquefaction of biomass (Anchusa azurea) compared to other thermochemical conversion methods. Biomass Convers Biorefin. 2019;9(2): 459-470. doi:10.1007/s13399-019-00379-4
- 8. Chen WT, Haque MA, Lu T, Aierzhati A, Reimonn G. A perspective on hydrothermal processing of sewage sludge. Curr Opin Environ Sci Health. 2020;14:63-73. doi:10.1016/j.coesh.2020.02.008
- Qian L, Wang S, Savage PE. Hydrothermal liquefaction of sewage sludge under isothermal and fast conditions. Bioresour Technol. 2017; 232:27-34. doi:10.1016/j.biortech.2017.02.017
- 10. Li H, Lu J, Zhang Y, Liu Z. Hydrothermal liquefaction of typical livestock manures in China: biocrude oil production and migration of heavy metals. J Anal Appl Pyrolysis. 2018;135:133-140. doi:10.1016/j. jaap.2018.09.010
- 11. Chen J, Wang L, Zhang B, Li R, Shahbazi A. Hydrothermal liquefaction enhanced by various chemicals as a means of sustainable dairy manure treatment. Sustainability. 2018;10(1):230. doi:10.3390/su10010230
- 12. Katakojwala R, Kopperi H, Kumar S, Venkata MS. Hydrothermal liquefaction of biogenic municipal solid waste under reduced H2 atmosphere in biorefinery format. Bioresour Technol. 2020;310:123369. doi:10.1016/j.biortech.2020.123369
- 13. Kohansal K, Toor S, Sharma K, Chand R, Rosendahl L, Pedersen TH. Hydrothermal liquefaction of pre-treated municipal solid waste (biopulp) with recirculation of concentrated aqueous phase. Biomass Bioenergy. 2021;148:106032. doi:10.1016/j.biombioe.2021.106032
- 14. Seshasayee MS, Savage PE. Synergistic interactions during hydrothermal liquefaction of plastics and biomolecules. Chem Eng J. 2021;417: 129268. doi:10.1016/j.cej.2021.129268
- 15. Raikova S, Knowles TDJ, Allen MJ, Chuck CJ. Co-liquefaction of macroalgae with common marine plastic pollutants. ACS Sustain Chem Eng. 2019;7(7):6769-6781. doi:10.1021/acssuschemeng.8b06031
- 16. Energy & Fuels. Combined Hydrothermal Liquefaction of Polyurethane and Lignocellulosic Biomass for Improved Carbon Recovery. Accessed April 26, 2022. https://pubs.acs.org/doi/abs/10.1021/acs. energyfuels.1c01520
- 17. Yu J, Biller P, Mamahkel A, et al. Catalytic hydrotreatment of biocrude produced from the hydrothermal liquefaction of aspen wood: a catalyst screening and parameter optimization study. Sustain Energy Fuels. 2017;1(4):832-841. doi:10.1039/C7SE00090A
- 18. Bai B, Jin H, Fan C, Cao C, Wei W, Cao W. Experimental investigation on liquefaction of plastic waste to oil in supercritical water. Waste Manag. 2019;89:247-253. doi:10.1016/j.wasman.2019.04.017
- 19. Oliveux G, Dandy LO, Leeke GA. Current status of recycling of fibre reinforced polymers: review of technologies, reuse and resulting properties. Prog Mater Sci. 2015;72:61-99. doi:10.1016/j.pmatsci. 2015.01.004
- 20. Shibasaki Y, Kamimori T, Kadokawa J, Hatano B, Tagaya H. Decomposition reactions of plastic model compounds in sub- and supercritical

GHALANDARI ET AL.

AICHE 10 of 11
IOURNAI

- water. Polym Degrad Stab. 2004;83(3):481-485. doi:10.1016/j.polymdegradstab.2003.09.010
- Damodharan D, Sathiyagnanam AP, Rana D, Rajesh Kumar B, Saravanan S. Extraction and characterization of waste plastic oil (WPO) with the effect of n-butanol addition on the performance and emissions of a DI diesel engine fueled with WPO/diesel blends. *Energ Convers Manage*. 2017;131:117-126. doi:10.1016/j.enconman.2016.10.076
- 22. Jie H, Ke H, Wenjie Q, Zibin Z. Process analysis of depolymerization polybutylene terephthalate in supercritical methanol. *Polym Degrad Stab.* 2006;91(10):2527-2531. doi:10.1016/j.polymdegradstab
- Saha N, Banivaheb S, Toufiq RM. Towards solvothermal upcycling of mixed plastic wastes: Depolymerization pathways of waste plastics in sub- and supercritical toluene. *Energy Convers Manag.* 2022;13: 100158. doi:10.1016/j.ecmx.2021.100158
- Lee LS, H Jung O, H Ling H. The experiments and correlations of the solubility of ethylene in toluene solvent. *Fluid Phase Equilib*. 2005; 231(2):221-230. doi:10.1016/j.fluid.2005.02.010
- Sangon S, Ratanavaraha S, Ngamprasertsith S, Prasassarakich P. Coal liquefaction using supercritical toluene–tetralin mixture in a semicontinuous reactor. Fuel Process Technol. 2006;87(3):201-207. doi:10. 1016/j.fuproc.2005.07.007
- Chang HZ, Li JQ, Du S, et al. Transformation characteristics of hydrogen-donor solvent tetralin in the process of direct coal liquefaction. Front Chem. 2019;7:737.
- Faba L, Díaz E, Ordóñez S. Hydrodeoxygenation of acetone–furfural condensation adducts over alumina-supported noble metal catalysts. *Appl Catal Environ*. 2014;160-161:436-444. doi:10.1016/j.apcatb.2014.05.053
- Yan P, Mensah J, Drewery M, Kennedy E, Maschmeyer T, Stockenhuber M. Role of metal support during ru-catalysed hydrodeoxygenation of biocrude oil. Appl Catal Environ. 2021;281:119470. doi:10.1016/j.apcatb.2020.119470
- Jia C, Xie S, Zhang W, et al. Deconstruction of high-density polyethylene into liquid hydrocarbon fuels and lubricants by hydrogenolysis over Ru catalyst. Chem Catal. 2021;1(2):437-455. doi:10.1016/j.checat.2021.04.002
- Oya S, Kanno D, Watanabe H, Tamura M, Nakagawa Y, Tomishige K. Catalytic production of branched small alkanes from biohydrocarbons. ChemSusChem. 2015;8(15):2472-2475. doi:10.1002/cssc.201500375
- 31. Sinfelt JH. Specificity in catalytic hydrogenolysis by metals. In: Eley DD, Pines H, Weisz PB, eds. *Advances in Catalysis*. Vol 23. Academic Press; 1973:91-119. doi:10.1016/S0360-0564(08)60299-0
- Shu R, Xu Y, Ma L, et al. Hydrogenolysis process for lignosulfonate depolymerization using synergistic catalysts of noble metal and metal chloride. RSC Adv. 2016;6(91):88788-88796. doi:10.1039/ C6RA16725J
- Ahmad MM, Nordin MFR, Azizan MT. Upgrading of bio-oil into high-value hydrocarbons via hydrodeoxygenation. Am J Appl Sci. 2010; 7(6):746-755. doi:10.3844/ajassp.2010.746.755
- Duan P, Savage PE. Hydrothermal liquefaction of a microalga with heterogeneous catalysts. *Ind Eng Chem Res.* 2011;50(1):52-61. doi:10. 1021/ie100758s
- Seshasayee MS, Savage PE. Oil from plastic via hydrothermal liquefaction: production and characterization. Appl Energy. 2020;278: 115673. doi:10.1016/j.apenergy.2020.115673
- ScienceDirect. Upcycling and Catalytic Degradation of Plastic wastes. Accessed April 26, 2022. https://www.sciencedirect.com/science/article/pii/S2666386421002186
- Shakya R, Adhikari S, Mahadevan R, Hassan EB, Dempster TA. Catalytic upgrading of bio-oil produced from hydrothermal liquefaction of Nannochloropsis sp. Bioresour Technol. 2018;252:28-36. doi:10.1016/j.biortech.2017.12.067
- Nanayakkara S, Patti AF, Saito K. Chemical depolymerization of lignin involving the redistribution mechanism with phenols and repolymerization of depolymerized products. Green Chem. 2014;16(4):1897-1903. doi:10.1039/C3GC41708E

- Alberti C, Enthaler S. Depolymerization of end-of-life poly(bisphenol A carbonate) via alkali-metal-halide-catalyzed methanolysis. Asian J Org Chem. 2020;9(3):359-363. doi:10.1002/ajoc.201900242
- Li L, Li Y, Fang Z, He C. Study on molecular structure characteristics of natural dissolved organic nitrogen by use of negative and positive ion mode electrospray ionization Orbitrap mass spectrometry and collision-induced dissociation. *Sci Total Environ*. 2022;810:152116. doi:10.1016/j.scitotenv.2021.152116
- 41. Liu Y, Chandra Akula K, Phani Raj Dandamudi K, et al. Effective depolymerization of polyethylene plastic wastes under hydrothermal and solvothermal liquefaction conditions. *Chem Eng J.* 2022;446:137238. doi:10.1016/j.cej.2022.137238
- Bai X, Duan P, Xu Y, Zhang A, Savage PE. Hydrothermal catalytic processing of pretreated algal oil: a catalyst screening study. Fuel. 2014; 120:141-149. doi:10.1016/j.fuel.2013.12.012
- Nizamuddin S, Baloch HA, Mubarak NM, et al. Solvothermal liquefaction of corn stalk: physico-chemical properties of bio-oil and biochar. Waste Biomass Valorization. 2019;10(7):1957-1968. doi:10. 1007/s12649-018-0206-0
- Nizamuddin S, Jaya Kumar NS, Sahu JN, Ganesan P, Mubarak NM, Mazari SA. Synthesis and characterization of hydrochars produced by hydrothermal carbonization of oil palm shell. *Can J Chem Eng.* 2015; 93(11):1916-1921. doi:10.1002/cjce.22293
- Baloch HA, Siddiqui MTH, Nizamuddin S, et al. Effect of solvent on hydro-solvothermal co liquefaction of sugarcane bagasse and polyethylene for bio-oil production in ethanol-water system. *Process Saf Environ Prot*. 2021;148:1060-1069. doi:10.1016/j.psep.2021.02.015
- Park J, Won SW, Mao J, Kwak IS, Yun YS. Recovery of Pd(II) from hydrochloric solution using polyallylamine hydrochloride-modified Escherichia coli biomass. J Hazard Mater. 2010;181(1):794-800. doi: 10.1016/j.jhazmat.2010.05.083
- Nolte MW, Shanks BH. A perspective on catalytic strategies for deoxygenation in biomass pyrolysis. *Energ Technol.* 2017;5(1):7-18. doi:10. 1002/ente.201600096
- Shiraishi Y, Hirakawa H, Togawa Y, Hirai T. Noble-metal-free deoxygenation of epoxides: titanium dioxide as a photocatalytically regenerable electron-transfer catalyst. ACS Catal. 2014;4(6):1642-1649. doi:10.1021/cs500065x
- Khan S, Kay Lup AN, Qureshi KM, Abnisa F, Wan Daud WMA, Patah MFA. A review on deoxygenation of triglycerides for jet fuel range hydrocarbons. J Anal Appl Pyrolysis. 2019;140:1-24. doi:10. 1016/j.jaap.2019.03.005
- 50. Liu B, Wang Z, Feng L. Effects of reaction parameter on catalytic hydrothermal liquefaction of microalgae into hydrocarbon rich bio-oil. *J Energy Inst*. 2021;94:22-28. doi:10.1016/j.joei.2020.10.008
- Ratha SK, Renuka N, Abunama T, Rawat I, Bux F. Hydrothermal liquefaction of algal feedstocks: the effect of biomass characteristics and extraction solvents. *Renew Sustain Energy Rev.* 2022;156:111973. doi: 10.1016/j.rser.2021.111973
- Li C, Zhang X, Hao X, et al. Efficient recovery of high-purity aniline from aqueous solutions using pervaporation-fractional condensation system. AIChE J. 2015;61(12):4445-4455. doi:10.1002/aic.15006
- 53. Ro KS, Venugopal A, Adrian DD, et al. Solubility of 2,4,6-trinitrotoluene (TNT) in water. *J Chem Eng Data*. 1996;41(4): 758-761. doi:10.1021/je950322w
- Bowers JS Jr. Toluidines. In: Ullmann CF, ed. Ullmann's Encyclopedia of Industrial Chemistry. John Wiley & Sons, Ltd; 2000. doi:10.1002/ 14356007.a27_159
- Abodif AM, Meng L, S MA, et al. Mechanisms and models of adsorption: TiO₂-supported biochar for removal of 3,4-dimethylaniline. ACS Omega. 2020;5(23):13630-13640. doi:10.1021/acsomega.0c00619
- Kalauz A, Kapui I. Determination of potentially genotoxic impurities in crotamiton active pharmaceutical ingredient by gas chromatography.
 J Pharm Biomed Anal. 2022;210:114544. doi:10.1016/j.jpba.2021. 114544

5475905, 2022, 12, Downloaded from https://aiche.onlinelibrary.wiley.com/doi/10.1002/aic.17863, Wiley Online Library on [28/12/2022]. See the Terms and Conditions (https://onlinelibrary.wiley.com/erms and-conditions) on Wiley Online Library for rules of use; OA articles are governed by the applicable Creative Commons License

- Mimura N, Saito M. Dehydrogenation of ethylbenzene to styrene over Fe2O3/Al2O3 catalysts in the presence of carbon dioxide. *Catal Today*. 2000;55(1):173-178. doi:10.1016/S0920-5861(99)00236-9
- Nikolov V, Klissurski D, Anastasov A. Phthalic anhydride from oxylene catalysis: science and engineering. *Catal Rev.* 1991;33:319-374. doi:10.1080/01614949108020303
- Fan X, Du B. Selective detection of trace p-xylene by polymer-coated QCM sensors. Sens Actuators B Chem. 2012;166-167:753-760. doi: 10.1016/j.snb.2012.03.060
- Xiu FR, Qi Y, Wang S, Nie W, Weng H, Chen M. Application of critical water-alcohol composite medium to treat waste printed circuit boards: oil phase products characteristic and debromination. *J Hazard Mater*. 2018;344:333-342. doi:10.1016/j.jhazmat.2017.10.033
- Huang J, Sun N, Dong Y, et al. Similar or totally different: the control of conjugation degree through minor structural modifications, and deep-blue aggregation-induced emission luminogens for non-doped OLEDs. Adv Funct Mater. 2013;23(18):2329-2337. doi:10.1002/ adfm.201202639
- Full article: Fluorene based organic dyes for dye sensitised solar cells: structure-property relationships. Accessed April 27, 2022. https://www.tandfonline.com/doi/full/10.1179/1753555712Y.0000000036
- 63. Bernius M, Inbasekaran M, Woo E, Wu W, Wujkowski L. Fluorenebased polymers-preparation and applications. *J Mater Sci Mater Electron*. 2000;11(2):111-116. doi:10.1023/A:1008917128880
- Yemam HA, Mahl A, Tinkham JS, Koubek JT, Greife U, Sellinger A. Highly soluble p-terphenyl and fluorene derivatives as efficient dopants in plastic scintillators for sensitive nuclear material detection. *Chem A Eur J.* 2017;23(37):8921-8931. doi:10.1002/chem.201700877
- 65. Xie F, Zhang T, Bryant P, Kurusingal V, Colwell JM, Laycock B. Degradation and stabilization of polyurethane elastomers. *Prog Polym Sci.* 2019;90:211-268. doi:10.1016/j.progpolymsci.2018.12.003
- 66. Bao JL, Zheng J, Truhlar DG. Kinetics of hydrogen radical reactions with toluene including chemical activation theory employing system-specific

- quantum RRK theory calibrated by variational transition state theory. J Am Chem Soc. 2016;138(8):2690-2704. doi:10.1021/jacs.5b11938
- Haryńska A, Kucinska-Lipka J, Sulowska A, Gubanska I, Kostrzewa M, Janik H. Medical-grade PCL based polyurethane system for FDM 3D printing—characterization and fabrication. *Materials*. 2019;12(6):887. doi:10.3390/ma12060887
- Kluson P, Cerveny L. Selective hydrogenation over ruthenium catalysts.
 Appl Catal Gen. 1995;128(1):13-31. doi:10.1016/0926-860X(95)00046-1
- Kamsuwan T, Jongsomjit B, Herrera JE. The role of ruthenium on the acidity of mixed alumina and silica phases and its impact on activity for ethanol dehydration. *Can J Chem Eng.* 2022;100(3):559-568. doi: 10.1002/cjce.24147
- Dang HLT, Tran NA, Dao VD, et al. Carbon nanotubes-ruthenium as an outstanding catalyst for triiodide ions reduction. Synth Met. 2020; 260:116299. doi:10.1016/j.synthmet.2020.116299
- Hamid MHSA, Williams JMJ. Ruthenium catalysed N-alkylation of amines with alcohols. Chem Commun. 2007;7:725-727. doi:10.1039/ B616859K

SUPPORTING INFORMATION

Additional supporting information can be found online in the Supporting Information section at the end of this article.

How to cite this article: Ghalandari V, Banivaheb S, Peterson J, Smith H, Reza MT. Solvothermal liquefaction of waste polyurethane using supercritical toluene in presence of noble metal catalysts. *AIChE J.* 2022;68(12):e17863. doi:10. 1002/aic.17863